JASA ARTICLE

# Reduction of nonlinear distortion in condenser microphones using a simple post-processing technique

Petr Honzík[1,a] and Antonin Novak[2,b]
[1]Department of Radioelectronics, Faculty of Electrical Engineering, Czech Technical University in Prague, Technická 2, 166 27 Praha, Czech Republic
[2]Laboratoire d'Acoustique de l'Université du Mans (LAUM), UMR 6613, Institut d'Acoustique–Graduate School (IA-GS), Centre National de la Recherche Scientifique, Le Mans Université, Le Mans, France

**ABSTRACT:**
In this paper, an approach for effectively reducing nonlinear distortion in single-backplate condenser microphones is introduced, i.e., most microelectromechanical systems (MEMS) microphones, studio recording condenser microphones, and laboratory measurement microphones. This simple post-processing technique can be easily integrated on external hardware such as an analog circuit, microcontroller, audio codec, digital signal processing unit, or within the Application Specific Integrated Circuit chip in a case of MEMS microphones. It effectively reduces microphone distortion across its frequency and dynamic range, and relies on a single parameter, which can be derived from either the microphone's physical parameters or a straightforward measurement presented in this paper. An optimal estimate of this parameter achieves the best distortion reduction, whereas overestimating it never increases distortion beyond the original level. The technique was tested on a MEMS microphone. The findings indicate that for harmonic excitation, the proposed technique reduces the second harmonic by approximately 40 dB, leading to an effective reduction in the total harmonic distortion. The efficiency of the distortion reduction technique for more complex signals is demonstrated through two-tone and multitone experiments, where second-order intermodulation products are reduced by at least 20 dB.  https://doi.org/10.1121/10.0035579

(Received 24 September 2024; revised 28 December 2024; accepted 9 January 2025; published online 3 February 2025)

[Editor: Michael J. White] Pages: 699–705

## I. INTRODUCTION

Condenser microphones, including MEMS (microelectromechanical systems) microphones, are widely used in various applications because of their high sensitivity, wide frequency response, and compact size.[1] However, nonlinear distortion,[2] which affects audio quality and measurement accuracy, presents two challenges: it is difficult to measure accurately[3,4] and even more difficult to reduce effectively.[5–8]

Nonlinear distortion in microphones manifests itself as unwanted harmonic[9] and intermodulation[10] products, which affect the acquisition accuracy of the acoustic pressure signal. This distortion arises from a number of sources,[11] which include mechanical properties of the diaphragm,[12] variations in air gap damping between the membrane and backplate as a result of thickness changes, acoustic nonlinearities caused by high acoustic pressure in the air gap, cavity stiffness, preamplifier characteristics, and the nonlinear capacitance change of the microphone capsule.[9] Among these sources, the nonlinear capacitance change is considered to be the primary contributor to distortion in condenser microphones. According to Djuric,[13] the second harmonic, which is associated with quadratic nonlinearity of the microphone, contributes close to 90% of the total harmonic distortion (THD).

MEMS microphones, which have gained popularity in recent years for their integration into mobile devices and acoustic measurement systems, are inherently susceptible to nonlinear distortion because of their small size and unique construction. Previous studies have shown that the nonlinear behavior of MEMS microphones can significantly affect the accuracy of acoustic measurements, particularly at high sound pressure levels (SPLs).[14,15]

Despite the advancements in microphone technology, addressing nonlinear distortion remains an important area of research. One approach to achieving a reduction of the second harmonic in single-backplate microphones is to insert a negative capacitance in the preamplifier circuit.[5] Fletcher and Thwaites[6] suggest reducing nonlinear distortion by using a shallow parabolic backplate, although this method introduces manufacturing complications. Another technique for reducing distortion caused by the nonlinear behavior of condenser microphone capsules is the implementation of "dual backplate" technology.[7] This method uses two backplates to reduce the nonlinear effects associated with changes in capsule capacitance but is generally more expensive as a result of increased complexity and manufacturing issues. In addition, a method applicable exclusively to complementary metal-oxide semiconductor (CMOS) MEMS microphones

[a]Email: honzikp@fel.cvut.cz
[b]Email: antonin.novak@univ-lemans.fr

exploits the capacitance-voltage nonlinear characteristics of a P-type metal-oxide-semiconductor capacitor to address MEMS nonlinearity at the Application Specific Integrated Circuit (ASIC) level.[8]

In this context, the present study introduces a novel post-processing technique that has the potential to significantly reduce distortion levels of all single-backplate condenser type microphones. This easy-to-implement technique can be integrated into various hardware configurations, including analog circuits, microcontrollers, audio codecs, digital signal processing (DSP) units, and ASIC chips for MEMS microphones.

The paper is structured as follows. In Sec. II, we provide an overview of microphones distortion and its measurement technique used in this work. Section III A elaborates on the model of the distortion in condenser microphones employed in our study. In Sec. III B, we present the proposed technique in detail, highlighting its simplicity and feasibility. Finally, Sec. IV presents the measurement results, demonstrating how effectively the proposed method reduces microphone distortion.

## II. MICROPHONE DISTORTION MEASUREMENT

Measuring the distortion of microphones poses significant challenges, particularly, in the absence of linear sources. In our research, we use a recently published method,[16] enabling us to measure and analyze the distortion of microphones at high-pressure levels, as detailed further in this section.

The measurement setup employed in this work involves two identical 6.5" loudspeakers placed face to face, separated by a 2 cm high plastic cylindrical piece with a central aperture and a volume of approximately $10^{-5}$ m$^3$ (see Fig. 1). These loudspeakers are connected in parallel to create a push-push configuration, which generates pressure excitation inside the aperture with a low distortion. The MEMS microphone under test and the reference 1/8" Pressure Microphone GRAS 40DP (Holte, Denmark) are positioned approximately 1 mm apart within the center of the aperture. Note that the MEMS microphone used in this study is an arbitrarily chosen single back plate microphone available on the market (CUI devices, CMM-2718AB-38308-TR, Lake Oswego, OR). The supply voltage used here is 3.3 V. Similar results and conclusions were obtained for other single-backplate MEMS microphones.

The signal generation and acquisition are managed using an RME Fireface 400 sound card (Haimhausen, Germany). A sine signal is sent from the sound card to the loudspeakers, which generates the sound pressure inside the aperture. The output of the microphone under test is connected directly to the sound card input while the reference microphone is connected through a GRAS 26AC preamplifier and Brüel and Kjær type 2609 conditioning amplifier (Nærum, Denmark). To ensure a pure harmonic excitation inside the aperture, we apply the nonlinear harmonic correction technique.[16] As a result, the pressure signal inside the

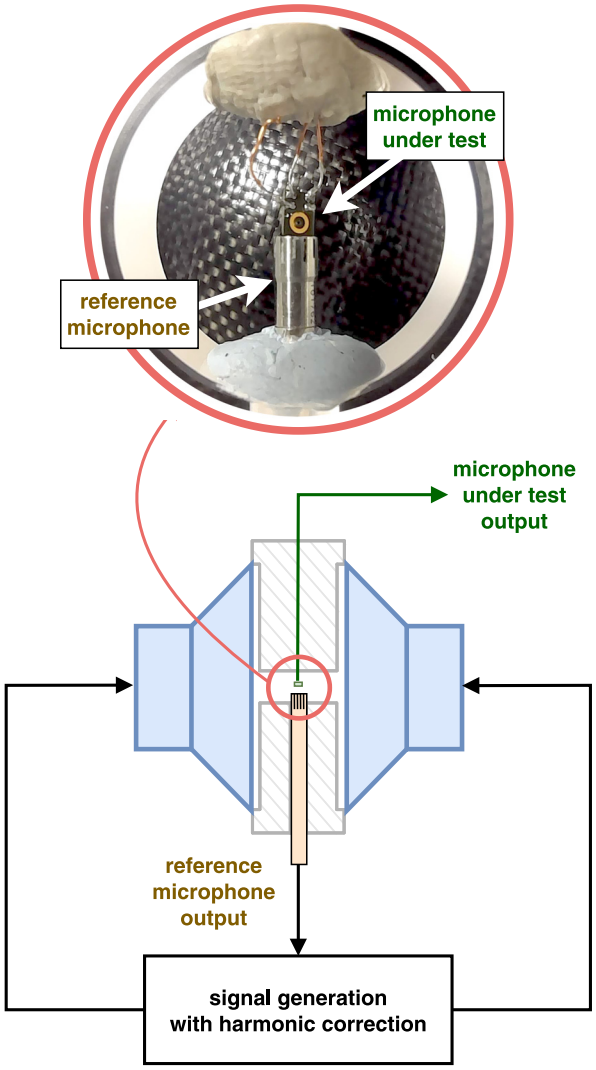


FIG. 1. Schematic view of the measurement setup.

aperture, measured by the reference microphone—whose distortion is negligible at the measured SPLs—contains no unwanted higher harmonics or intermodulation products as these components are effectively suppressed to the noise level. This measurement procedure is repeated for excitation levels ranging from 85 to 128 dB SPL.

Figure 2 shows an example of the spectra of the measured sound pressure for a 1 kHz excitation at a level of 116 dB SPL. Figure 2(a) presents the efficiency of the applied harmonic correction. The higher harmonics measured by the reference microphone are suppressed to the noise level, resulting in a pure harmonic excitation inside the aperture (this remains valid at all of the measured levels from 85 to 128 dB SPL). Figure 2(b) shows the spectra of the sound pressure simultaneously measured by the microphone under test. Note that the thermal noise of the reference microphone is approximately 52 dB(A) SPL according to the datasheet, whereas the thermal noise of MEMS microphones is typically below 30 dB(A) SPL.

The results of such a measurement are displayed in Fig. 3. The measured levels of the first harmonic (blue

https://doi.org/10.1121/10.0035579

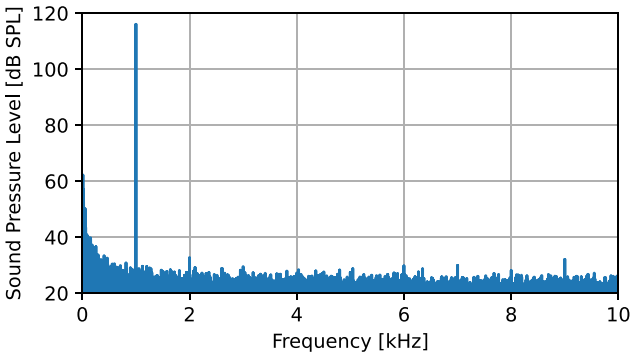


(a) reference microphone

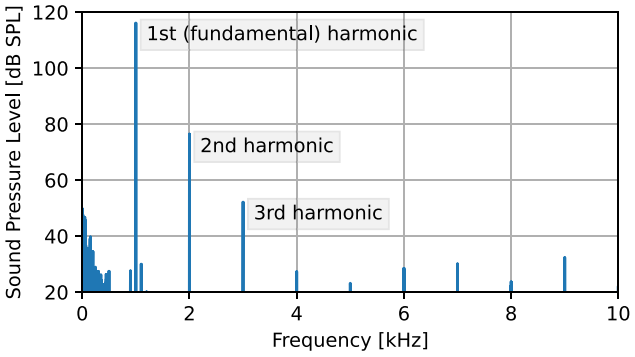


(b) microphone under test

FIG. 2. Example of spectra of the measured sound pressure with the (a) reference microphone and (b) MEMS microphone under test. Note that attributed to the harmonic correction, there are no higher harmonics measured by the reference microphone.

points), second harmonic (orange points), and third harmonic (green points) at the output of the MEMS microphone under test are shown for a 1 kHz excitation. These levels are recalculated to an equivalent input SPL through the measured sensitivity of the MEMS microphone. The results are depicted as a function of SPL measured by the reference microphone. The theoretical levels of the harmonic components, given by the model described below, are represented by dashed lines of corresponding colors. Up to approximately 120 dB SPL, the second harmonic fits the predicted

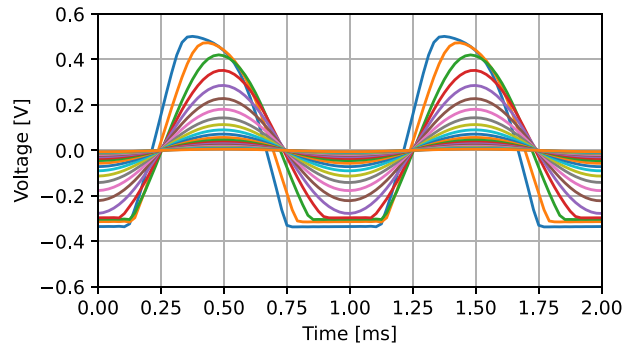


FIG. 4. Time-domain signal of the voltage at the output of the microphone under test for different levels of the incident pressure. Note that the electrical signals for the four highest SPLs (122, 124, 126, and 128 dB SPL) are saturated.

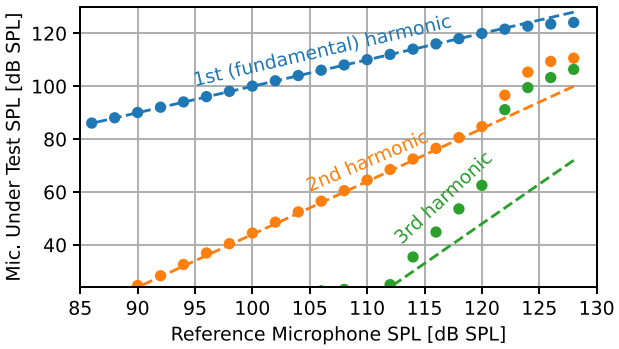


FIG. 3. SPL of first three harmonics for the microphone under test as a function of reference SPL. Measurement results are denoted by dots, and model results are depicted by dashed lines.

value well, whereas the third harmonic is several dBs higher. This discrepancy is likely caused by acoustic nonlinearities inside the microphone, such as variations in air gap damping due to thickness changes and acoustic nonlinearities caused by high acoustic pressure in the air gap, which are not accounted for in the model. This observation is consistent with previously published research.[14,17] Above 120 dB SPL, the microphone output signal presents asymmetric clipping (see Fig. 4), probably originating from the electronic part of the microphone, and the measured data cannot be predicted by the model at these levels.

## III. TECHNIQUE FOR REDUCTION OF DISTORTION

### A. Model of condenser microphone distortion

In this section, we provide a concise summary of the nonlinear model of a single-backplate condenser microphone.[14]

The relationship between the output voltage $u(t)$ and the change in capacitance $\mathrm{d}C(t)$ can be expressed as

$$u(t) = -U_0 \frac{\mathrm{d}C(t)}{C}, \tag{1}$$

where $U_0$ represents the polarization voltage, and the distortion is caused by nonlinear behavior of the capacitance change $\mathrm{d}C(t)$. Equation (1) can be further expanded to the following expression:

$$u(t) = U_0 \frac{C_0}{C_P + C_0} \left[ \frac{\bar{\xi}(t)}{h_g} - \left( \frac{\bar{\xi}(t)}{h_g} \right)^2 + \left( \frac{\bar{\xi}(t)}{h_g} \right)^3 - \cdots \right], \tag{2}$$

where $C_P$ represents the parasitic capacitance, $C_0$ is the static capacitance of the microphone, $h_g$ denotes the air gap thickness between the membrane and backplate, and $\bar{\xi}$ represents the mean displacement of the membrane over the backplate area. Equation (2) can be rewritten as

$$u(t) = K_0 \left[ y(t) - y^2(t) + y^3(t) - \cdots \right], \tag{3}$$

where $K_0$ represents a constant that depends on the capacitance and polarization voltage

$$K_0 = U_0 \frac{C_0}{C_P + C_0}, \tag{4}$$

and $y$ represents the relative mean membrane displacement with respect to the air gap thickness. Equation (3) provides a simplified form to model the distortion characteristics in the electrical output of the condenser microphone.

### B. Reduction of distortion

As previously mentioned, the primary distortion component in single-backplate microphones is the second harmonic. Furthermore, recent work[14] has confirmed this finding for single-backplate MEMS microphones, showing that the abovementioned model accurately predicts this distortion component regardless of SPL and frequency. Consequently, the critical objective in distortion reduction is to effectively suppress, mainly, the quadratic component. Therefore, we can preserve the powers of $y(t)$ up to the second order in Eq. (3), leading to

$$u(t) = K_0\left[y(t) - y^2(t)\right]. \tag{5}$$

The procedure for distortion reduction through inversion of Eq. (5) is described in this section.

First, we denote $u_{\text{lin}}(t) = K_0 y(t)$ as the distortion free output signal. Then, the output voltage given by Eq. (5) becomes

$$u(t) = u_{\text{lin}}(t) - \frac{1}{K_0} u_{\text{lin}}^2(t), \tag{6}$$

and one can find an inverse function to Eq. (6), providing an estimate of the linear output signal as

$$u_{\text{lin}}(t) = \frac{K_0}{2}\left[1 - \sqrt{1 - \frac{4u(t)}{K_0}}\right]. \tag{7}$$

Using Taylor series expansion around zero, the estimate of the linear output signal given by Eq. (7) can be further simplified to

$$u_{\text{lin}}(t) \approx u(t) + \frac{1}{K_0} u^2(t). \tag{8}$$

A block schema for such a distortion reduction technique is depicted in Fig. 5.

The constant $K_0$ [the only parameter necessary for the reduction of distortion using Eqs. (7) or (8)] can be calculated from the polarization voltage $U_0$ and the static ($C_0$) and parasitic ($C_P$) capacitances of the microphone [see Eq. (4)]. Because these parameters are not always known, a simple method for estimation of $K_0$ is proposed later.

Considering a pure harmonic excitation of the microphone membrane at the frequency $f_0$, the mean displacement to air gap thickness ratio can be described by $y(t) = y_m \sin(2\pi f_0 t)$, where $y_m$ denotes the amplitude. The absolute values of the first and second components of the Fourier series of the nonlinear output $u(t)$ [Eq. (5)] can be expressed, respectively, as $V_1 = K_0 y_m$, corresponding to frequency $f_0$, and $V_2 = K_0 y_m^2/2$, corresponding to frequency $2f_0$. The constant $K_0$, thus, can be estimated from these measured spectral components

$$K_0 = \frac{V_1^2}{2V_2}. \tag{9}$$

Such an estimate is independent of input excitation level and frequency. Figure 6 shows the estimate of $K_0$ according to Eq. (9) for different input levels at 1 kHz (blue points) using the measured data from Fig. 3, resulting in an estimated coefficient value of $K_0 = 8.85$ V (gray dashed line). Note that if a gain $G$ is applied to the output of the microphone before the correction procedure, then $GK_0$ must be used instead of $K_0$.

## IV. RESULTS

In this section, the performance of the proposed distortion reduction technique is studied for different types of input signals. The impact of incorrect estimation of the parameter $K_0$ is also discussed.

### A. Harmonic distortion

First, the microphone was excited by a pure sine tone, which led to the presence of higher harmonics at its output due to the distortion, as shown in Fig. 7 (blue line). Then, the distortion reduction technique has been applied on the microphone output signal, resulting in a significant reduction of the second harmonic component of the output signal spectrum; see the orange line in Fig. 7 (shifted to left for clarity). The upper graph of Fig. 7 shows the result when applying the complete inverse function given by Eq. (7), and the lower graph presents the result of the simplified Eq. (8). In both cases, the second harmonic component is reduced by approximately 40 dB, whereas the other harmonics stay almost intact (the slight increase in the third harmonic in the lower graph is negligible). Because Eq. (8) provides very similar results to Eq. (7) with lower computational costs, all of the following results are obtained using this simple technique.

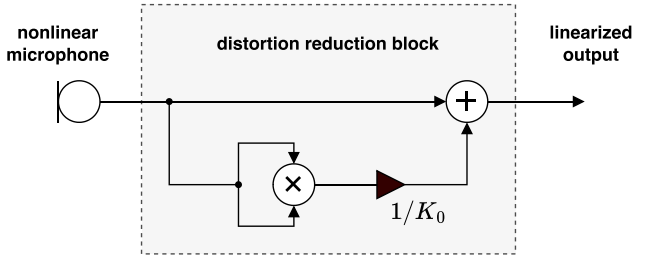


FIG. 5. Block schema of the proposed distortion reduction technique.

https://doi.org/10.1121/10.0035579

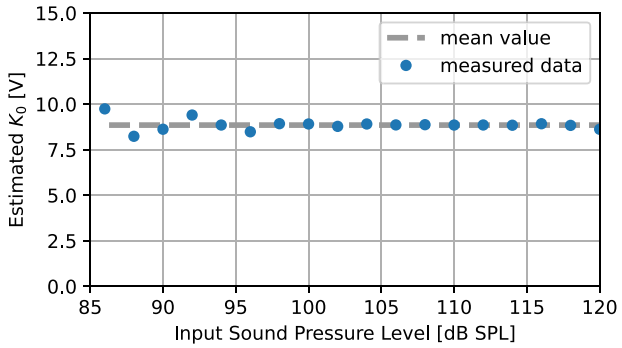


FIG. 6. Estimated value of the coefficient $K_0$ as a function of reference SPL. The measurement results are denoted by dots, and the selected optimal value $K_0$ is represented by the gray dashed line.

Figure 8 presents the THD of the microphone at 1 kHz without any post-processing (blue points) and when applying the distortion reduction technique (orange crosses) as a function of the input SPL. Except for very low levels, where the second harmonic is hidden in background noise, and very high levels, where signal clipping appears (the acoustic overload point, defined as the 10% THD level, appears near 123 dB SPL, which is contrary to the 130 dB SPL stated in the datasheet), THD is reduced 10 times near 120 dB SPL or even 50 times near 110 dB SPL. Note that the THD obtained using the distortion reduction technique never exceeds the original THD (without any processing).

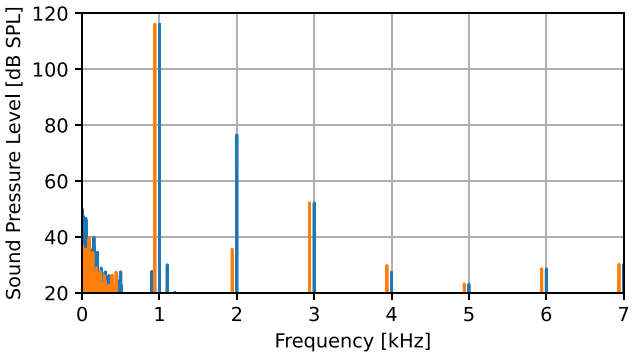


(a) Distortion reduction (eq. (7))

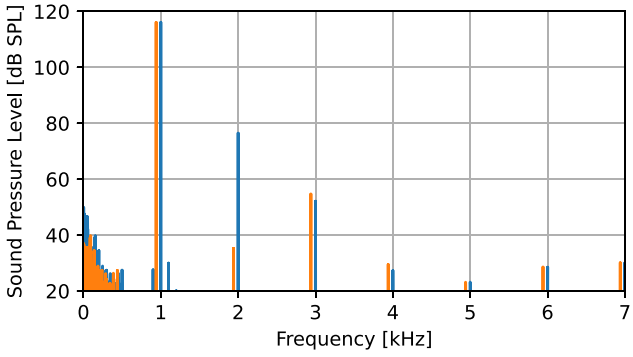


(b) Distortion reduction (eq. (8))

FIG. 7. Spectral analysis of microphone signal for 1 kHz excitation. The blue spectrum corresponds to the original (unprocessed) signal, the orange spectrum (shifted to the left) corresponds to the signal processed by the proposed technique [Eq. (7), upper graph and Eq. (8), lower graph].

### B. Impact of $K_0$ uncertainty

The reduction of distortion described above was achieved using the value of $K_0$, estimated with Eq. (9). However, if we use Eq. (4), including parameters $U_0$, $C_0$, and $C_P$, which may not all be known precisely, $K_0$ could be estimated inaccurately. To study the effect of uncertainty in $K_0$ on THD, we repeated the previous test for different values of $K_0$. Figure 9 shows the dependence of THD on the varying value of $K_0$ using Eq. (7) (orange stars) and Eq. (8) (green circles) compared to THD when no distortion reduction is applied (blue line) for input SPL of 110 dB SPL at 1 kHz. First, it is clear, again, that the difference between results of Eqs. (7) and (8) is negligible. Next, the estimated value of $K_0 = 8.85$ V from Eq. (9) (vertical dashed gray line in Fig. 9) fits well with the minimum THD value. Furthermore, Fig. 9 shows that although the best distortion reduction is achieved with the optimal estimated value of $K_0$, THD is reduced to some extent in very large range of values of $K_0$. However, if the value of $K_0$ is largely underestimated (below 50% of the optimal value), the THD can exceed its original value. On the other hand, overestimating the value of $K_0$ by 50% still leads to a reduction of THD by a factor of 2. Indeed, overestimating the value of $K_0$ never causes the increase in THD above the level obtained without any distortion reduction. This is obvious from Eq. (8), where the quadratic term decreases with increasing $K_0$ and the result $u_{\mathrm{lin}}(t)$ converges to the original distorted signal $u(t)$.

### C. Intermodulation distortion

To evaluate the robustness of the proposed method under intermodulation distortion, two complex signals are used to excite the microphone: (i) a two-tone signal consisting of 1440 Hz and 1680 Hz components with a total root mean square (RMS) value of 8 Pa, corresponding to 109 dB SPL for each component; and (ii) a multitone signal consisting of 100 Hz, 300 Hz, 500 Hz, 1 kHz, 1.8 kHz, 3.4 kHz, 6.1 kHz, 11.1 kHz, and 20 kHz components with a total RMS value of 5 Pa, corresponding to approximately 98.5 dB

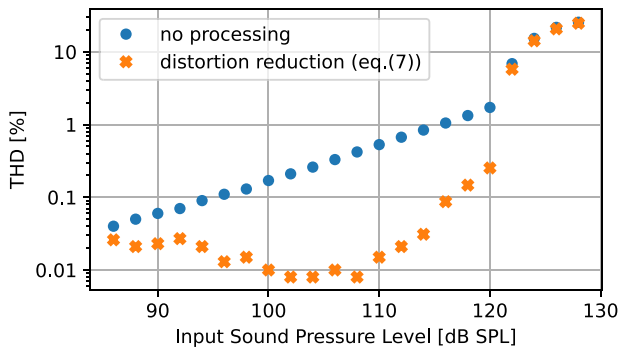


FIG. 8. THD as a function of reference SPL at 1 kHz. The unprocessed values are represented by blue dots, and the values after applying distortion reduction are denoted by orange crosses.

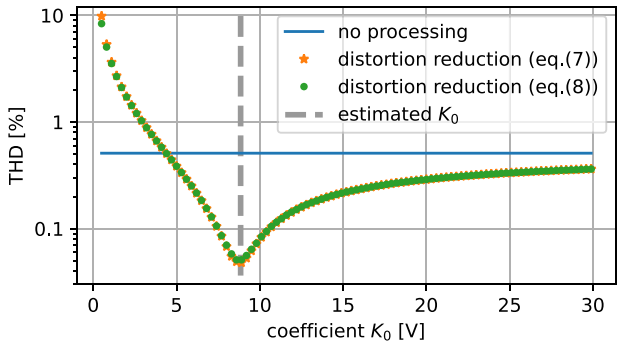


FIG. 9. THD of the MEMS microphone at 1 kHz and 110 dB SPL plotted as a function of the coefficient $K_0$. The unprocessed value is represented by the blue line, the technique applying the distortion reduction from Eq. (7) is shown by the orange stars, and the technique applying the distortion reduction from Eq. (8) is depicted by the green circles.

SPL for each component. All spectral components in both signals have random phases to improve the crest factor.[18] The harmonic correction technique,[16] previously used for single sine excitation, is also employed here to ensure pure two-tone and multitone excitation. This technique is applicable to any periodic signal and effectively ensures that only the desired spectral components are present.

Figure 10 depicts the spectrum of resulting signal when applying the distortion reduction technique (orange line) and without any distortion reduction (blue line). The upper graph shows the result for the two-tone signal, where the second-order harmonics and intermodulation products at 240, 2880, 3120, and 3360 Hz are reduced by more than 25 dB. For the multitone signal, the intermodulation products are reduced by approximately 20 dB, on average, as shown in the lower graph.

## V. CONCLUSION

In conclusion, this paper presents a new technique aimed at reducing nonlinear distortion in single-backplate condenser microphones, e.g., MEMS microphones. The proposed technique offers a simple and efficient solution, requiring minimal post-processing that can be easily implemented on an ASIC chip or in external hardware (analog circuit, microcontroller, audio codec, DSP unit, etc.) and reduces the microphone distortion within its frequency and dynamic range.

One of the key advantages of this technique is its reliance on a single parameter, $K_0$, which can be deduced either from the microphone physical parameters (polarisation voltage, static and parasitic capacitance) or a straightforward measurement. With a correct estimation of the parameter $K_0$, the THD can be reduced by a factor of 10 or even a factor of 50, depending on excitation level. Remarkably, even an incorrect estimation of $K_0$ by 50% still leads to substantial reductions in THD, highlighting the robustness of this approach.

The method has very low computational cost, requiring only two multiplications and one addition per sampling period, making its contribution to signal post-processing latency negligible. As the algorithm does not involve feedback, stability issues are not expected, even in the presence of rounding errors. However, care must be taken when implementing the square of large signals in Eq. (8) as this may lead to arithmetic overflow on certain hardware platforms (in this case, the multiplication by $1/\sqrt{K_0}$ can be performed prior to the square calculation).

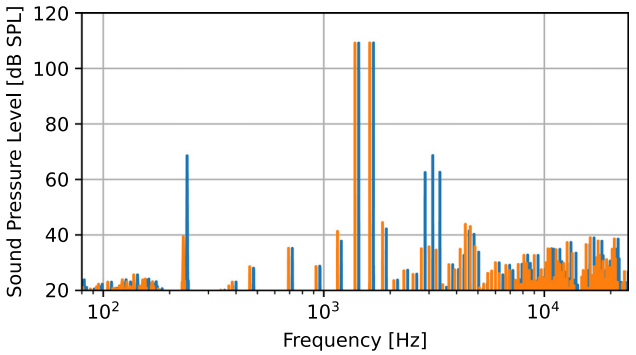


(a) two-tone excitation

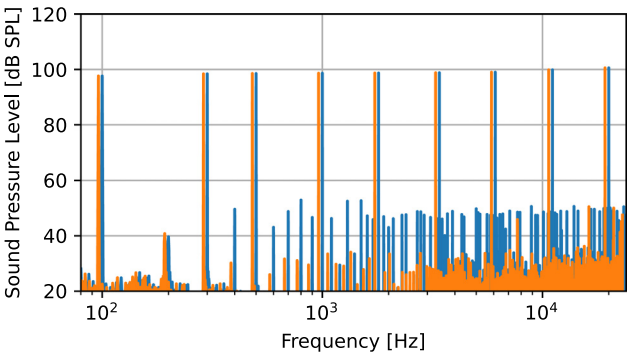


(b) multitone excitation

FIG. 10. Spectral analysis of microphone signal for a two-tone (upper graph) and multi-tone (lower graph) excitation. The blue spectrum corresponds to the original (unprocessed) signal, and the orange spectrum (shifted to the left) corresponds to the signal processed by the proposed technique.

The efficiency of the distortion reduction technique of more complex signals is demonstrated through two-tone and multitone experiments. Both experiments show an important reduction of intermodulation components created by the microphone at around 20 dB. This finding further strengthens the reliability and applicability of the proposed technique.

Considering the ease of implementation, low-cost nature, and robustness of this method, it holds great promise for improving the performance of single-backplate microphones, including MEMS microphones.

## ACKNOWLEDGMENTS

This work was supported by Project No. 23-07621J of the Czech Science Foundation (GAČR) "Otoacoustic emissions in normal cochlea and cochlea with endolymphatic hydrops: Modeling and experiments," by the

Grant Agency of the Czech Technical University in Prague, Grant No. SGS23/185/OHK3/3T/13 and the IA-GS, Le Mans, France. A patent application for this invention has been filed with the French National Institute of Industrial Property (INPI) under Application No. FR2404994 on May 16, 2024.

## AUTHOR DECLARATIONS

### Conflict of Interest

The authors have no conflicts to disclose.

## DATA AVAILABILITY

The data that support the findings of this study are available from the corresponding author upon reasonable request.

[1]M. Fueldner, "Chapter 48—Microphones," in *Handbook of Silicon Based MEMS Materials and Technologies, 3rd ed.*, edited by M. Tilli, M. Paulasto-Krockel, M. Petzold, H. Theuss, T. Motooka, and V. Lindroos (Elsevier, New York, 2020), pp. 937–948.
[2]S. Yoshikawa, "Study on the linearity of laboratory standard condenser microphone," J. Acoust. Soc. Am. **83**(S1), S63 (1988).
[3]E. Frederiksen, "System for measurement of microphone distortion and linearity at very high sound levels," J. Acoust. Soc. Am. **110**, 2670 (2001).
[4]H. Dahlke and G. T. Kantarges, "Investigation of microphone nonlinearities, using the high-intensity pistonphone," J. Acoust. Soc. Am. **40**, 1248 (1966).
[5]E. Frederiksen and W. Bolton, "Reduction of non-linear distortion in condenser microphones by using negative load capacitance," in *Proceedings of Internoise 96*, Liverpool, UK (June 30–August 2, 1996), pp. 2679–2684, available at https://www.ingentaconnect.com/contentone/ince/incecp/1996/00001996/00000003/art00040.
[6]N. H. Fletcher and S. Thwaites, "Electrode surface profile and the performance of condenser microphones," J. Acoust. Soc. Am. **112**(6), 2779–2785 (2002).
[7]M. Füldner and A. Dehé, "Dual back plate silicon MEMS microphone: Balancing high performance!," in *Proceedings of the DAGA 2015*, Nürnberg, Germany (March 16–19, 2015) [Deutsche Gesellschaft für Akustik e.V. (DEGA), Berlin, 2015], pp. 41–43.
[8]M. Nikolić, W. Florian, R. Gaggl, and L. Liao, "A 125dbspl 1%-thd, 115$\mu a$ MEMS microphone using passive pre-distortion technique," in *ESSCIRC 2023—IEEE 49th European Solid State Circuits Conference (ESSCIRC)*, Lisbon, Portugal (September 11–14, 2023) (IEEE, New York, 2023), pp. 209–212.
[9]H. Pastillé, "Electrically manifested distortions of condenser microphones in audio frequency circuits," J. Audio Eng. Soc. **48**(6), 559–563 (2000), available at https://secure.aes.org/forum/pubs/journal/?elib=12058.
[10]M. T. Abuelma'atti, "Improved analysis of the electrically manifested distortions of condenser microphones," Appl. Acoust. **64**(5), 471–480 (2003).
[11]A. Dessein, "Modelling distortion in condenser microphones," Ph.D. thesis, Technical University of Denmark, DTU, Lyngby, Denmark, 2009.
[12]S. Chowdhury, M. Ahmadi, and W. C. Miller, "Nonlinear effects in MEMS capacitive microphone design," in *Proceedings of the International Conference on MEMS, NANO and Smart Systems, ICMENS 2003*, Banff, AB, Canada (July 23, 2003) (IEEE, New York, 2003), pp. 297–302, available at https://ieeexplore.ieee.org/document/1222013.
[13]S. V. Djuric, "Distortion in microphones," in *ICASSP'76. IEEE International Conference on Acoustic Speech and Signal Processing*, Philadelphia, PA (April 12–14, 1976) (IEEE, New York, 1976), Vol. 1, pp. 537–539, available at https://ieeexplore.ieee.org/document/1169943.
[14]A. Novak and P. Honzík, "Measurement of nonlinear distortion of mems microphones," Appl. Acoust. **175**, 107802 (2021).
[15]G. Printezis, N. Aage, and F. Lucklum, "A non-dimensional time-domain lumped model for externally DC biased capacitive microphones with two electrodes," Appl. Acoust. **216**, 109758 (2024).
[16]A. Novak, L. Simon, and P. Lotton, "A simple predistortion technique for suppression of nonlinear effects in periodic signals generated by nonlinear transducers," J. Sound Vib. **420**, 104–113 (2018).
[17]A. Novak and P. Honzík, "Measurement of microphone harmonic distortion using predistortion technique," in *Proceedings Forum Acusticum*, Turin, Italy (September 11–15, 2023) (EAA, Torino, Italy, 2023).
[18]S. Temme and P. Brunet, "A new method for measuring distortion using a multitone stimulus and noncoherence," J. Audio Eng. Soc. **56**(3), 176–188 (2008), available at https://secure.aes.org/forum/pubs/journal/?ID=4.